

Safe Control of Arbitrary Nonlinear Systems using Dynamic Extension

Yihang Yao, Tianhao Wei, Changliu Liu

Abstract—Safe control for control-affine systems has been extensively studied. However, due to the complexity of system dynamics, it is challenging and time-consuming to apply these methods directly to non-control-affine systems, which cover a large group of dynamic systems, such as UAVs and systems with data-driven Neural Network Dynamic Models (NNDMs). Although all dynamic systems can be written in control-affine forms through dynamic extension, it remains unclear how to optimally design a computationally efficient algorithm to safely control the extended system. This paper addresses this challenge by proposing an optimal approach to synthesize safe control for the extended system under the framework of energy-function-based safe control. The proposed method first extends the energy function and then performs hyperparameter optimization to maximize performance while guaranteeing safety. It has been theoretically proved that our method guarantees safety (forward invariance of the safe set) and performance (bounded tracking error and smoother trajectories). It has been numerically validated that the proposed method is computationally efficient for non-control-affine systems.

I. INTRODUCTION

Safety is one of the most important factors in many robot applications. For example, we need to ensure safety of drivers and vehicles in autonomous driving, keep workers and robot arms safe in factories, and protect Unmanned Aerial Vehicles (UAVs) from collisions with obstacles.

A safe control law should ensure forward invariance of a user-defined safe set. To realize safe control, a form of scalar energy function-based approaches was proposed [1], [2], [3]. The energy function is defined such that the safe states are with low energy, while the control law should ensure energy dissipation. Quadratic programming (QP)-based control using energy function is widely applied in safe control tasks [4], [5]. These methods require that the systems dynamics are control-affine in order to reduce the overall problem into quadratic optimizations, so as to achieve efficient online computation. However, many dynamics are not control-affine, such as UAV dynamics and data-driven Neural Network Dynamic Models (NNDMs).

Recently, several safe control methods have been proposed for non-control-affine systems. One line of work is through direct optimization, e.g., nonlinear model predictive control (NMPC) with control barrier function (CBF) [6], [7]; Another line of work is through stochastic learning, e.g., Reinforcement Learning for safe control [8], [9]. However, direct optimization is computationally inefficient, while stochastic

learning is sample inefficient. It remains unclear how to develop computationally efficient and sample-efficient safe control algorithms for arbitrary nonlinear systems.

The key insight that this paper leverages is that any dynamic system can be written as a control-affine form through dynamic extension (DE). Hence we can derive safe control for the extended control-affine systems, where the nonlinear optimization associated with arbitrary nonlinear dynamics reduces to quadratic optimization, which can then be computed efficiently online. DE is a common method for nonlinear system control, e.g., in feedback linearization [10], [11]. In literature, it has been used to convert non-control-affine dynamics to control-affine dynamics in order to apply existing safe control techniques [12]. However, existing work focuses on the design of the safe control after DE. It remains unclear whether safe control after DE will result in any inefficiency compared to safe control without DE, and if so, how to optimize the safe control after DE to balance the gain in the computation efficiency and the loss of performance.

This paper studies how to optimally design a computationally efficient algorithm to safely control the extended system, under the framework of energy-function-based safe control. We assume that there is already a valid (but computationally inefficient) safe control law for the original system. The goal is to optimally “extend” that safe control law with respect to the extended system. To achieve that, we first study how to extend the safe control law such that safety can still be assured after dynamic extension. In particular, we study both input tracking and state tracking problems, which cover most cases for motion control problems. Secondly, we propose an optimization method to automatically choose the best hyperparameters for the extended safe control, which can improve the feasibility of safe control (by enlarging the safe control sets for different states) under DE. Lastly, for general nonlinear systems we analyze how the extension affects the computational efficiency and safety, how to provide theoretical guarantees of global attractiveness and forward invariance of the safe set, the smoothness of safe control with DE, and the bounded tracking error with DE.

II. NOTATION AND PROBLEM FORMULATION

A. Systems

As shown in Fig. 1, We consider the following discrete time non-control-affine system¹ with m states and n inputs:

$$x_{k+1} = x_k + \Delta x_k T_S, \text{ where } \Delta x_k := f(x_k, u_k), \quad (1)$$

¹Our methods and theoretical analysis also work for continuous-time systems by taking the limit of sampling time to zero. But to emphasize our contribution without loss of generality, we use the discrete-time system, which leads to more universal theoretical results.

Y. Yao, T. Wei and C. Liu are with the Robotics Institute, Carnegie Mellon University, PA, USA (email: {yihangy, twei2, cliu6}@andrew.cmu.edu).

Y. Yao is with the School of Mechanical Engineering, Shanghai Jiao Tong University, Shanghai, China (email: yaoyihang@sjtu.edu.cn).

where T_S is the sampling time, k is the time step, $x_k \in \mathcal{X}_b \subseteq \mathbb{R}^m$ is the state vector defined in the configuration space, and $u_k \in \mathcal{U}_b \subset \mathbb{R}^n$ is the input vector assumed to be constrained. We redefine Δx as the finite time difference and the right derivative of x . For safe tracking control, $u_k^r \in \mathbb{R}^n$ is the reference control and $x_k^r \in \mathbb{X}^m$ is the reference state.

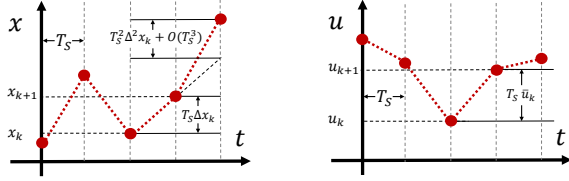


Fig. 1: Evolution of the system

B. Safety constraints

The safety constraint requires the system state to stay in a user-defined safe set \mathcal{X}_0 , which is a closed subset of the state space. \mathcal{X}_0 can be defined by a zero-sublevel set of a continuous and piecewise smooth function $\phi_0 : \mathbb{R}^m \rightarrow \mathbb{R}$, i.e., $\mathcal{X}_0 = \{x \mid \phi_0(x) \leq 0\}$. The design of ϕ_0 is usually straightforward. For example, for collision avoidance, ϕ_0 can be designed as the negative distance between the obstacle and the ego robot plus some margin. However, it may not always exist a control law to make \mathcal{X}_0 forward invariant or globally attractive. That is, the system state may inevitably leave \mathcal{X}_0 due to dynamic limits. Therefore, under the energy function based safe control methods, we need to design a new energy function $\phi(x) : \mathbb{R}^m \rightarrow \mathbb{R}$ such that 1) safe states are with low energy; 2) there always exists a feasible control to dissipate the energy when it is unsafe. We define the zero-sublevel set of ϕ by $\mathcal{X}_S = \{x \mid \phi(x) \leq 0\}$.

As shown in [13], the energy function transforms the safety constraint in the state space to a constraint in the control space such that

$$\dot{\phi} \leq -\eta(\phi), \quad (2)$$

where η is a tunable function on ϕ . Then, the safe control set for the state x is defined as:

$$\mathcal{U}(x) := \{u \in \mathcal{U}_b \mid \dot{\phi}(x) \leq -\eta(\phi)\}. \quad (3)$$

In this work, we define the function $\eta(\phi)$ as

$$\eta(\phi) = \lambda \cdot \phi + \delta, \quad (4)$$

where λ and δ are both functions on ϕ , and when $\phi \geq 0$, we require $\lambda \geq 0$ and $\delta \geq 0$ to ensure energy dissipation. As the definition of λ and δ change, the method fits into different common safe control algorithms, and ensures safety for continuous systems. For example, the Safe Set Algorithm (SSA) [2] indicates that: $\lambda = 0$, $\delta = -\infty$ if $\phi < 0$ and $\delta > 0$ if $\phi \geq 0$; the Barrier Function Method (BFM) [4] indicates that $\lambda > 0$, $\delta = 0$; and the Sub-level Safe Set (SSS) [13] indicates that $\delta = 0$, $\lambda = -\infty$ if $\phi < 0$ and $\lambda > 0$ if $\phi \geq 0$.

Common methods for constructing such ϕ include analytical methods [2], numerical methods [14], and learning

methods [15]. Previous methods are introduced for continuous time control, but in this work, we use it in discrete time under the assumption that the T_s is small. And because we focus on extending an existing safe control law. We assume a good ϕ is already given.

Assumption 1. With T_S being sufficiently small, and defining $\dot{\phi} = \frac{\partial \phi}{\partial x} \Delta x$ as the right time derivative of ϕ , control law (2) guarantees the safety for discrete-time systems as well.

Assumption 2. A good $\phi(x)$ is given for the nonlinear system in (1) such that the following safe set

$$\mathcal{S}_1 := \mathcal{X}_S \cap \mathcal{X}_0 \quad (5)$$

is forward invariant (the safe control law keeps the system state in the safe set when it is safe) and globally attractive (the safe control law drives the system back to the safe set when it is unsafe) with the Safe Set Algorithm.

C. Optimization-based safe control

In the optimization-based safe control framework, an input-tracking problem is formulated as

$$\min_{u_k \in \mathcal{U}(x)} \|u_k - u_k^r\|, \quad (6)$$

and a state-tracking problem is formulated as

$$\min_{u_k \in \mathcal{U}(x)} \|\Delta x_k - \Delta x_k^r\|. \quad (7)$$

Safe control is calculated at each time step k .

D. Dynamics Extension

In this paper, DE is applied to convert non-control-affine systems into control-affine forms. By defining the extended state as $\bar{x}_k := [x_k^T, u_k^T]^T \in \bar{\mathcal{X}}_b \subset \mathbb{R}^{m+n}$ and the extended control as $\bar{u}_k := \Delta u_k = \frac{u_{k+1} - u_k}{T_S} \in \bar{\mathcal{U}}_b \subset \mathbb{R}^n$, $\bar{\mathcal{U}}_b(x_k, u_k) = \left\{ \Delta u \mid \Delta u = \frac{u_{k+1} - u_k}{T_S}; u_{k+1} \in \mathcal{U}_b \right\}$, the system dynamics become control-affine:

$$\bar{x}_{k+1} = \bar{x}_k + \Delta \bar{x}_k T_S, \quad \Delta \bar{x}_k = \underbrace{\begin{bmatrix} f(x_k, u_k) \\ 0 \end{bmatrix}}_{\bar{f}(\bar{x}_k)} + \underbrace{\begin{bmatrix} 0 \\ 1 \end{bmatrix}}_{\bar{g}} \bar{u}_k. \quad (8)$$

III. METHODS

In this section, we discuss how to use our methods to reformulate and efficiently solve the constrained optimization problems presented in (6) and (7). Firstly, we extend the energy function by adding a derivative term. Then we derive hyperparameter design rules to ensure the forward invariance of safe set and safe control feasibility. Lastly, we propose a hyperparameter optimization method to improve the feasibility of the safe control with DE and select hyperparameters automatically for general nonlinear systems.

A. Extending the energy function

Assumption 3. The function $\phi(x)$ is L_1 -smooth, the function $f(x, u)$ is L_2 -smooth and uniformly bounded as $\|f\| \leq f_{max}$.

The original energy function ϕ does not work with DE, mainly because the relative degree from ϕ to \bar{u} is greater than one. Hence we extend the energy function by including the first-order derivative of ϕ :

$$\bar{\phi} := \phi + K(\dot{\phi} + \epsilon), \quad (9)$$

where $K > 0$, and constant $\epsilon = \frac{1}{2}L_1f_{max}^2T_S^2$ is introduced to tolerate discrete-time approximation error.

The extended sublevel safe set is defined as

$$\bar{\mathcal{X}}_S := \{[x, u] \mid \bar{\phi} \leq 0; \phi \leq 0\}. \quad (10)$$

The projection of the extended sublevel safe set $\bar{\mathcal{X}}_S$ on the state space \mathbb{R}^m is defined as

$$\bar{\mathcal{X}}_e := \{x_k \mid [x_k, u_k] \in \bar{\mathcal{X}}_S\}. \quad (11)$$

It is clear that $\bar{\mathcal{X}}_e$ is a subset of \mathcal{X}_S , i.e., $\bar{\mathcal{X}}_e \subseteq \mathcal{X}_S$ by the definition in (10). We will discuss the control set that guarantees the global attractiveness and forward invariance of the safe set with the following assumption.

Assumption 4. The constraints of the original inputs u introduced by $u \in \mathcal{U}_b$ is defined in a linear form:

$$\mathcal{U}_b = \{u \mid L u \leq S\}, \quad (12)$$

where L is a constant matrix and S is a constant vector.

Denote $\ddot{\phi} := \frac{\partial \dot{\phi}}{\partial x} \Delta x + \frac{\partial \dot{\phi}}{\partial u} \bar{u}$ as the right time derivative of $\dot{\phi}$, where $\frac{\partial \dot{\phi}}{\partial x} = \frac{\partial^2 \phi}{\partial x^2} \Delta x + \frac{\partial \phi}{\partial x} \frac{\partial f}{\partial x}$, and $\frac{\partial \dot{\phi}}{\partial u} = \frac{\partial \phi}{\partial x} \frac{\partial f}{\partial u}$, then $\ddot{\phi} = \dot{\phi} + K\ddot{\phi}$. The extended safe control set, which is state dependent, is defined as

$$\begin{aligned} \bar{\mathcal{U}}(\bar{x}) := & \{\bar{u} \mid \dot{\phi} \leq -\eta(\bar{\phi}); \bar{u} \in \bar{\mathcal{U}}_b\} \\ & = \{\bar{u} \mid \hat{L}(t) \bar{u} \leq \hat{S}(t)\} \end{aligned} \quad (13)$$

The projection of the extended safe control set on the input space \mathbb{R}^n is defined as

$$\bar{\mathcal{U}}_e(\bar{x}) := \{u_{k+1} \mid u_{k+1} = u_k + \bar{u}_k T_S; \bar{u}_k \in \bar{\mathcal{U}}\} \quad (14)$$

We will show in theorem 4 that with condition (21) - (23), the extended safe control set (13) is non-empty for control-affine systems, and in theorem 1 that any control law which is constrained by (13) will ensure the global attractiveness and forward invariance of the safe set

$$\mathcal{S}_2 = \bar{\mathcal{X}}_e \cap \mathcal{X}_0. \quad (15)$$

Hence, $\bar{\mathcal{X}}_S \cap \mathcal{X}_0$ is also forward invariant and globally attractive according to the definition of (10).

B. Formulation of safe control with DE

For the extended system, (6) and (7) need to be modified since the states and inputs have changed. Additionally, as the system is being extended, a one-step delay is introduced in the control objective function as shown in (19). To formulate the new tracking laws, we have to first keep the same objectives. The new tracking targets at time step k for input-tracking and state-tracking are defined as

$$\bar{u}_k^r = \frac{u_k^r - u_k}{T_S}, \quad \Delta^2 x_k^r = \frac{\Delta x_k^r - \Delta x_k}{T_S}. \quad (16)$$

Then, we introduce the objective functions. For the input-tracking problems, the optimization is designed in a similar form as (6) by replacing u with \bar{u} ,

$$\min_{\bar{u}_k \in \bar{\mathcal{U}}(\bar{x})} \|\bar{u}_k - \bar{u}_k^r\| \quad (17)$$

However, for the state-tracking problems, we cannot simply replace x with \bar{x} because the information of u_k^r in \bar{x}^r is unknown. Calculating u_k^r directly is computational expensive for arbitrary nonlinear systems. Instead, with denoting $\Delta^2 x_k := \Delta x'_+(t) = \frac{\partial f}{\partial x} \Delta x + \frac{\partial f}{\partial u} \bar{u} = \frac{\Delta x_{k+1} - \Delta x_k}{T_S}$ as the right time derivative of Δx , we can define the new tracking object as minimizing

$$\|\Delta^2 x_k - \Delta^2 x_k^r\| = \left\| \frac{\partial f}{\partial x} \Delta x_k + \frac{\partial f}{\partial u} \bar{u}_k - \Delta^2 x_k^r \right\|, \quad (18)$$

which is equivalent to the following form

$$\min_{\bar{u}_k \in \bar{\mathcal{U}}(\bar{x})} \|\Delta x_{k+1} - \Delta x_k^r\|. \quad (19)$$

C. Hyperparameter design rules

The hyperparameters λ , δ , K , and the sampling time T_S need to be carefully designed to ensure safety (global attractiveness and forward invariance of safe set \mathcal{S}_2 defined in (15)) and control feasibility of the system. Here we provide a design rule to ensure the safety for general nonlinear systems. But for control feasibility, it is difficult to derive a practical condition that guarantees the feasibility for arbitrary nonlinear systems because of the diversity of system dynamics. Therefore, we design a learning based method to improve the feasibility for general nonlinear systems in section III-D. And we give a design rule for control-affine systems to gain some intuition and help us initialize the optimization. The conditions for general nonlinear system control feasibility is left for future work.

Assumption 5. Function $\bar{\phi}(\bar{x})$ is L_3 -smooth, and Δu is bounded as $\|\Delta u\| \leq \bar{u}_{max}$.

Although we have already assumed Δu is bounded in (13), we suppose the norm of Δu is limited in an explicit way to make the following rules, theorems and proofs clearer. The design rules are shown as follows.

a) Design rule for safety: For general nonlinear systems and a well-defined energy function ϕ , suppose the control feasibility is guaranteed by the optimization process which will be introduced later in section III-D, the safety of safe set

\mathcal{S}_2 , including global attractiveness and forward invariance, is guaranteed by the condition that

$$\delta > \delta_0 = \frac{1}{2}L_3(f_{max}^2 + \bar{u}_{max}^2)T_S, \quad (20)$$

The proof is shown in theorem 1.

b) Design rule for feasibility: For a well-defined energy function ϕ and given parameters λ and δ , suppose the dynamic system is control-affine i.e., $f(x, u) = f^x(x) + f^u(x) u$, a sufficient condition for K and T_S to guarantee feasibility, i.e., $\bar{\mathcal{U}}(\bar{x}_k) \neq \emptyset$ for all \bar{x}_k after the extension is

$$\frac{1}{K} - \frac{T_S}{K^2} \leq \lambda < \frac{1}{T_S}, \quad (21)$$

$$K > T_S, \quad (22)$$

$$\delta \geq \frac{KT_S}{K - T_S}(\gamma_1 + \gamma_2 + \lambda\epsilon), \quad (23)$$

where γ_1 is the upper bound of $\frac{\partial \dot{\phi}}{\partial x} f$, and γ_2 is the upper bound of $(\lambda K - 1 + \frac{T_S}{K})\dot{\phi}$, i.e.,

$$\gamma_1 \geq \frac{\partial \dot{\phi}}{\partial x} f, \quad \gamma_2 \geq (\lambda K - 1 + \frac{T_S}{K})\dot{\phi}. \quad (24)$$

The proof is shown in theorem 4.

D. Optimization process

For general nonlinear systems f , we introduce a learning-based method to maximize the feasibility as well as to find the optimal hyperparameters $(K^*, \lambda^*, \delta^*)$ to achieve safe control feasibility when safe control is activated, i.e., $\bar{\phi} \geq 0$. The cost objective is designed as

$$J = J(K, \lambda, \delta) = \frac{\sum_{i=1}^s \Theta(\bar{x}_i)}{s} + C_1 K^2 + \frac{C_2}{\lambda^2} + \frac{C_3}{\delta^2}, \quad (25)$$

where the first term penalizes the infeasible rate, s is the sampling size, \bar{x}_i is the sampled extended state, and Θ is an indicator function of the non-feasibility of each sampling point. Denote $\bar{\mathcal{U}}_i$ as the extended safe control set at \bar{x}_i , then $\Theta(\bar{x}_i)$ is defined as

$$\Theta(\bar{x}_i) = \begin{cases} 0 & \text{if } \bar{\mathcal{U}}_i \neq \emptyset \\ 1 & \text{if } \bar{\mathcal{U}}_i = \emptyset \end{cases}. \quad (26)$$

The following terms in J are regularizers, where $C_1 \geq 0$, $C_2 \geq 0$, and $C_3 \geq 0$ are constant numbers introduced to speed up the convergence of optimization. More details about the optimization strategy are introduced in section V-B with a case study. The optimal hyperparameters are obtained by solving:

$$[K^*, \lambda^*, \delta^*] = \underset{K > 0, \lambda > 0, \delta > \delta_0}{\operatorname{argmin}} J \quad (27)$$

IV. THEORETICAL ANALYSIS

This section discusses the theoretical results. As shown in Fig. 2, for general nonlinear systems, when the safe control feasibility is ensured by optimization process in section III-D, theorem 1 guarantees the global attractiveness and forward invariance of the safe set, \mathcal{S}_2 in (11), and corollary 2 concludes the conservativeness of safe control with DE because the forward invariant set \mathcal{S}_2 in (11) is a subset of

\mathcal{S}_1 in (5). For control-affine systems, lemma 3 compares the safe boundary of input with and without DE and guarantees the features of safe control feasibility, smoothness of safe control, and bounded tracking error, which are proved in theorem 4, corollary 5, and theorem 6, respectively.

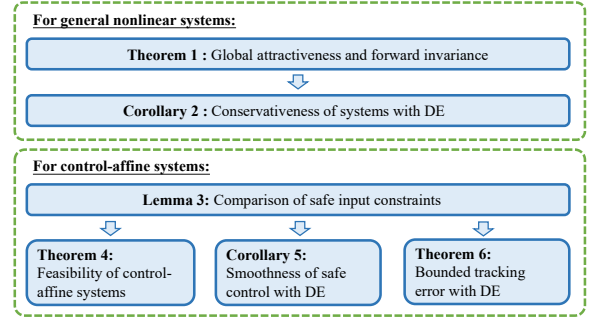


Fig. 2: Theorem diagram.

Before we claim theorem 1 and corollary 2, we have to make the following assumptions to guarantee the safe set is non-empty, and the safe control is always feasible.

Assumption 6. *The safe set \mathcal{S}_2 defined in (15) is non-empty.*

Assumption 7. *The optimization process presented in section III-D finds a set of hyperparameters that guarantees the safe control feasibility, i.e., set $\bar{\mathcal{U}}$ defined in (13) is non-empty everywhere.*

These assumptions hold empirically as shown in the experiments. For assumption 7, we can maximize the feasibility with our proposed optimization process by setting C_1, C_2, C_3 as 0, trying multiple initial values, and sampling densely.

Theorem 1. (Global attractiveness and forward invariance of safe set) *With assumption 6 and 7, the safe set \mathcal{S}_2 (11) is globally attractive and forward invariant.*

Proof. Though control law (13) indicates $\dot{\bar{\phi}} = -\delta < 0$ when $\bar{\phi} = 0$, discrete-time implementation weakens the forward invariance of set $\{\bar{\phi} \leq 0\}$ because $\bar{\phi}_{k+1} \neq \bar{\phi}_k + \dot{\bar{\phi}}_k T_S$. Firstly, we will show that with condition (20), the forward invariance of the set $\{\bar{\phi} \leq 0\}$ is ensured, i.e., when $\bar{\phi}_k = 0$, letting $\dot{\bar{\phi}}_k \leq -\delta$ leads to $\bar{\phi}_{k+1} < 0$.

Function $\bar{\phi}(\bar{x})$ is L_3 -smooth, i.e.,

$$\bar{\phi}(\bar{x}_{k+1}) \leq \bar{\phi}(\bar{x}_k) + \langle \nabla \bar{\phi}(\bar{x}_k), \bar{x}_{k+1} - \bar{x}_k \rangle + \frac{1}{2}L_3 \|\bar{x}_{k+1} - \bar{x}_k\|^2, \quad (28)$$

and the last term on the right side is bounded as

$$\frac{1}{2}L_3 \|\bar{x}_{k+1} - \bar{x}_k\|^2 \leq \frac{1}{2}L_3(f_{max}^2 + u_{max}^2)T_S^2. \quad (29)$$

the middle term on the right side is bounded as

$$\langle \nabla \bar{\phi}(\bar{x}_k), \bar{x}_{k+1} - \bar{x}_k \rangle = T_S \left(\frac{\partial \bar{\phi}}{\partial x} \Delta x_k + \frac{\partial \bar{\phi}}{\partial u} \Delta u_k \right) \leq -T_S \delta \quad (30)$$

Then, with (20), and (28)-(30), we get the conclusion that

$$\bar{\phi}_{k+1} < 0. \quad (31)$$

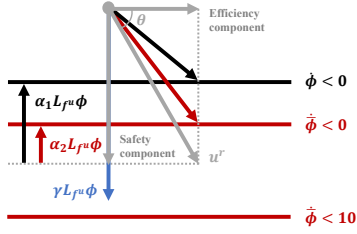


Fig. 3: Geometric interpretation of safe constraints in input space. The input can be decomposed into two parts: efficiency component and safety component [13]. Safe control with DE requires less change in inputs.

Thus the forward invariance of set $\{\bar{\phi} \leq 0\}$ is ensured. The following proof showing global attractiveness and forward invariance of \mathcal{S}_2 is validated with Fig. 4.

(a) global attractiveness of \mathcal{S}_2 :

- Condition 1 (area ①): At the initial time t_0 , $\bar{\phi}(t_0) > 0$: Under the safe control law (13), $\exists t_1 \in (t_0, \infty)$, s.t. $\bar{\phi}(t_1) \leq 0$, then the extended state goes to area ② or area ③.
- Condition 2 (area ②): $\bar{\phi}(t_0) \leq 0$, $\phi(t_0) > 0$: Since the definition or extended energy function is $\bar{\phi} = \phi + K(\dot{\phi} + \epsilon)$, then $\dot{\bar{\phi}} + \epsilon \leq -\frac{\dot{\phi}}{K}$, indicating that $\exists t_2 \in (t_0, \infty)$, s.t. $\dot{\bar{\phi}} \leq 0$, then the extended state goes to area ③.
- Condition 3 (area ③): $\bar{\phi}(t_0) \leq 0$, $\phi(t_0) \leq 0$: As the original energy function $\phi(t_0)$ is well-defined, $\exists t_3 \in (t_0, \infty)$, s.t. $\phi(t_3) \leq 0$ and $\phi_0(t_3) \leq 0$.

(b) Forward invariance of \mathcal{S}_2 :

- Condition 1 (boundary a): if $\phi_0 \leq 0$, $\phi \leq 0$, and $\bar{\phi} = 0$, then by control law (13), we get $\dot{\bar{\phi}} < -\delta$, and as shown in above, the forward invariance of $\{\bar{\phi} \leq 0\}$ is ensured.
- Condition 2 (boundary b): if $\phi_0 \leq 0$, $\phi = 0$, and $\bar{\phi} \leq 0$, then by $\dot{\bar{\phi}} = \dot{\phi} + K(\dot{\phi} + \epsilon) \leq 0$, $\dot{\bar{\phi}} < 0$.
- Condition 3 (boundary c): if $\phi_0 = 0$, $\phi \leq 0$, and $\bar{\phi} \leq 0$, then as safety energy function ϕ is well-defined, $\dot{\phi}_0 \leq 0$.

To conclude, the safe set \mathcal{S}_2 (11) is globally attractive and forward invariant. \square

Theorem 1 ensures the safety, including global attractiveness and forward invariance of the safe set \mathcal{S}_2 . In the next, the size of forward invariant safe sets \mathcal{S}_1 , and \mathcal{S}_2 are compared to evaluate the conservativeness of systems with DE.

Corollary 2. (Conservativeness of systems with DE) *With DE, the safe set \mathcal{S}_2 in (11) is a subset of the original one, \mathcal{S}_1 in (5), i.e., $\mathcal{S}_2 \subseteq \mathcal{S}_1$. And if $\dot{\phi} \neq 0$, it is a proper subset, i.e., $\mathcal{S}_2 \subset \mathcal{S}_1$.*

The relationship among safe sets is shown in Fig. 4. Corollary 2 shows that with the extended energy function in (9), the system is more conservative since the forward invariant safe set shrinks.

Lemma 3. (Comparison of safe input constraints) *Suppose the system is control-affine, i.e., $\Delta x = f(x, u) = f^x(x) + f^u(x) u$. When the safe control is activated, i.e., $\bar{\phi} \geq 0$, and the reference control is u_k^r . Then, with design rule (21)-(23),*

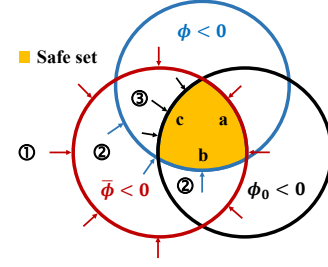


Fig. 4: The projection of safe sets on \mathbb{R}^m . Red arrows are induced by the safe control law (13), blue arrows exist by the definition of $\bar{\phi}$ (9), and black arrows exist according to the assumption that the original energy function ϕ ensures forward invariance and global attractiveness of \mathcal{S}_1 (5).

safe control is presented in the form $u_k = u_k^r - \alpha_1 L_{f^u} \phi$ for systems without DE and $u_{k+1} = u_k^r - \alpha_2 L_{f^u} \phi$ for systems with DE, where the index shift in the latter one is caused by the DE time delay. In addition, systems with DE have looser safety boundaries, i.e.,

$$\alpha_1 \geq \alpha_2, \quad (32)$$

The proof of theorem 3 is shown in appendix I. When the system is control-affine, lemma 3 indicates that 1) with DE, the safety constraint of input is also a half-space; 2) with DE, the safety restrictions are relaxed, i.e., $\mathcal{U}(x) \subseteq \bar{\mathcal{U}}_e(\bar{x})$ which leads to control feasibility, smoothness of safe control, and bounded tracking error as shown in theorem 4, corollary 5, and theorem 6, respectively.

Theorem 4. (Feasibility of safe control with DE) *Suppose the robot system is control-affine, i.e., $\bar{\phi} \geq 0$, and the safe control is activated, i.e., $\bar{\phi} \geq 0$. Then, with the design rule (21)-(23), the feasibility of safe control with DE is guaranteed.*

Proof. Since $\mathcal{U}(x) \subseteq \bar{\mathcal{U}}_e(\bar{x})$, and good ϕ implies that $\mathcal{U}(x) \neq \emptyset$ everywhere, then $\bar{\mathcal{U}}_e(\bar{x}) \neq \emptyset$, $\bar{\mathcal{U}}(\bar{x}) \neq \emptyset$ everywhere. \square

Theorem 4 indicates that for control-affine systems, the feasibility of safe control with DE is guaranteed. Additionally, it also shows that if the original system is not feasible everywhere for safe control, i.e., ϕ is not well-defined, DE and energy extension have the potential to increase the feasibility since $\mathcal{U}(x) \subseteq \bar{\mathcal{U}}_e(\bar{x})$. In the next, to evaluate the smoothness of input, we first define an indicator in the input space.

$$I^S = \frac{\langle u, L_{f^u} \phi \rangle}{\|u\| \cdot \|L_{f^u} \phi\|}, \quad (33)$$

where u is the safe control calculated at each time step k . For systems without DE, $u = u_k$, and for systems with DE, $u = u_{k+1}$. As shown in Fig. 3, the geometric interpretation of the indicator is

$$I^S = \sin(\theta) \quad (34)$$

Denote I_1^S as the indicator of systems without DE, and I_2^S as the indicator of systems with DE. Inspired by [13], $\sin(\theta)$ is the ratio of the safe component of the input. We choose

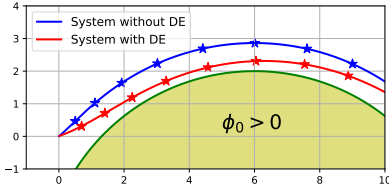


Fig. 5: Comparison of trajectories. The marked points are sampling points every 50 steps on the trajectories. Under the same λ and δ , DE makes the trajectories smoother and reduces the tracking error.

(34) as the indicator because when I^S is small, it indicates that the input needs to be revised sharply to satisfy the safety constraints, which makes the states change dramatically as well, resulting in rough trajectories. On the other hand, when I^S is large, the change of input and state is more moderate, thus the trajectory is smoother.

Corollary 5. (Smoothness of safe control with DE) *Suppose the robot system is control-affine, then with conditions (21)-(23), DE smooths the input for input-tracking problems, i.e.,*

$$I_2^S \geq I_1^S \quad (35)$$

Proof. Denote $\gamma = \frac{L_{fu}\phi^T u^r}{\|L_{fu}\phi\|^2}$, u^e as the input component orthogonal to the $L_{fu}\phi$, then

$$I^S = \sin(\theta) = \frac{\|(\gamma - \alpha_i)L_{fu}\phi^T u^r\|}{\|u^e + (\gamma - \alpha_i)L_{fu}\phi\|}, \quad (36)$$

since $\alpha_1 \geq \alpha_2$, then $I_2^S \geq I_1^S$. \square

Corollary 5 shows that DE revises the input smoothly to ensure safety. The trajectory with DE is also smoother as shown in Fig. 5. Besides the trajectory smoothness, the tracking error is also an important feature of safe control, which is studied in the next theorem.

Theorem 6. (Bounded tracking error with safety constraints) *Suppose the system is control-affine, and the tracking object Δx_k^r is dynamically feasible, then for state-tracking problems, the tracking error of Δx_k^r with DE is:*

$$\Delta = \Delta x_{k+1} - \Delta x_k^r = \Delta_1 + \Delta_2, \quad (37)$$

where Δ_1 comes from the discrete-time implementation, and Δ_2 comes from the safety constraint, and

$$\begin{cases} \|\Delta_1\| \leq \frac{L_2}{2} (f_{\max}^2 + \bar{u}_{\max}^2) T_S^2 \\ \Delta_2 = \alpha_2 f^u L_{fu} \phi \end{cases}. \quad (38)$$

The proof is shown in appendix II. Theorem 6 shows the tracking error is bounded with DE.

V. NUMERICAL STUDIES

The numerical studies are designed to answer the following questions:

(1) How do safe control methods with and without DE perform in terms of computational efficiency, smoothness of the trajectories, and tracking error with safety constraints?

(2) How does the hyperparameter optimization method proposed in section III-D improve the feasibility of the system with DE?

TABLE I. The comparison of state-tracking safe control with and without DE. A larger value of smoothness indicates the trajectory is smoother.

	Control-affine		Non-control-affine	
	w/o DE	w/ DE	w/o DE	w/ DE
Solving time	0.00050	0.00056	0.036	0.0037
Smoothness	-0.0177	-0.0134	-0.368	-0.204
Tracking error	1.89	1.45	2.87	2.31

To answer these questions, we design the following tasks. The first task is to perform safe control with and without DE on different systems. The second task is to compare the safe control under DE with and without hyperparameters optimization. We evaluate our method on analytical models (AMs) and NNDMs. The numerical studies are done on a computer with AMD® R7-4800H 8-core processor, 16 GB memory.

A. Safe control under DE

This task is designed to evaluate the performance of the safe control algorithm with and without DE in terms of computational efficiency, trajectory smoothness, and tracking error with safety constraints. Since theorem 6 is based on the control-affine assumption, both control-affine and non-control-affine systems are tested in this task. An analytical mobile agent model is chosen as the control-affine system, and a data-driven mobile agent model (NNDM) is chosen as the non-control-affine system. The smoothness of a trajectory is defined as

$$\text{Smoothness} = -\frac{\sum_{i=2}^n \kappa_i^2}{n-1}, \quad (39)$$

where κ_i is the curvature of the trajectory at time step i . This trajectory smoothness indicator is different from the one we proposed in (33) because indicator (33) compares the smoothness of safe controls at the same state to emphasize the effect of DE. But in practice, the states of the two trajectories are different, and the safe control is not activated all the time. We are interested in the smoothness of the whole trajectory.

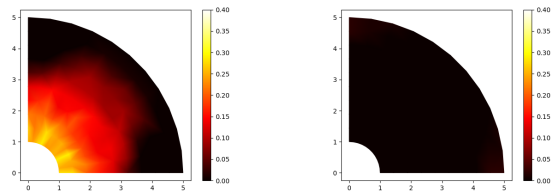
The results are shown in Table. I. DE method for safe control increases the smoothness of the trajectories, and reduces the tracking error with safety constraints for both affine and non-affine systems, and greatly accelerates the computation for non-control-affine systems.

B. Hyperparameter optimization

This task aims at evaluating the optimization method proposed in section III-D. An analytical model shown in appendix III is tested. This subsection will firstly show the optimization process, then the results.

1) *Optimization process:* A mobile agent system is chosen for examination. The cost function is defined in (25). We uniformly sampled the position, state, and input of the robot for evaluation. In this work, we use CMA-ES to search for the best solution for the hyperparameters.

The control-infeasible ring around the obstacle before and after hyperparameters optimization is shown in Fig. 6,



(a) Infeasible rate before hyperparameter optimization (b) Infeasible rate after hyperparameter optimization

Fig. 6: The control-infeasible rate around the obstacle. The obstacle is placed at the original point and its radius is 1. Since the result around the obstacle is symmetric, only a quarter of the ring area is presented. The infeasible rate drops significantly after the optimization.

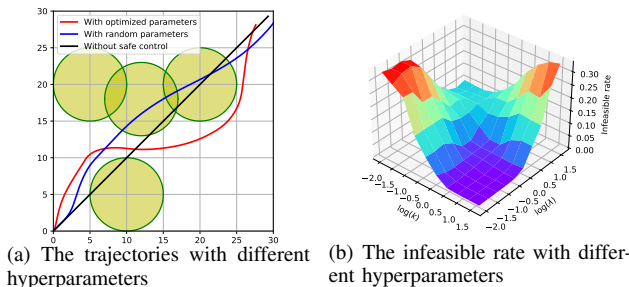


Fig. 7: With optimal hyperparameters, the systems can guarantee control feasibility, thus ensuring safety. Without the optimization, the feasibility rate is low, so the robot may crash into obstacles because the safe control is not feasible.

which indicates that the optimization process improves the feasibility of this system.

2) *Results comparison*: For result evaluation, the robot is asked to move from the start point to the end point. In every trial, a round obstacle is randomly generated on the map. The results of this experiment are concluded in table II. After optimization, the collision rate and infeasible rate decrease to zero. The comparison of systems with different parameters is shown in Fig. 7. The system with optimal hyperparameters behaves better.

VI. CONCLUSION AND FUTURE WORK

This paper aims at revealing the methodology and effects of DE in nonlinear system safe control. Both the system and energy function are extended to convert the safe control problems into QP problems. The theoretical analysis provides guarantees of global attractiveness and forward invariance of the safe set, smoothness of input, and bounded tracking error with safety constraints for the proposed algorithm.

TABLE II. The comparison of non-feasible rate R_N and collision rate R_C with optimized hyperparameters and random hyperparameters.

	Optimized	Random 1	Random 2
R_N	0	78%	22%
R_C	0	77%	22%

A hyperparameter optimization method is also proposed to select the hyperparameters automatically and improve the control-feasibility of systems with DE. Numerical studies are consistent with the theorems.

In the future work, we mainly consider two aspects: firstly, we will reveal the hyperparameter design rule for the general nonlinear systems to guarantee the safe control feasibility with DE; secondly, will extend the objective function to multi-step MPC.

REFERENCES

- [1] Rudolf E Kalman and John E Bertram. Control system analysis and design via the “second method” of lyapunov: I—continuous-time systems. 1960.
- [2] Changliu Liu and Masayoshi Tomizuka. Control in a Safe Set: Addressing Safety in Human-Robot Interactions. In *ASME 2014 Dynamic Systems and Control Conference*. American Society of Mechanical Engineers Digital Collection, 2014.
- [3] Quan Nguyen and Koushil Sreenath. Exponential control barrier functions for enforcing high relative-degree safety-critical constraints. In *2016 American Control Conference (ACC)*, pages 322–328. IEEE, 2016.
- [4] Aaron D Ames, Jessie W Grizzle, and Paulo Tabuada. Control barrier function based quadratic programs with application to adaptive cruise control. In *53rd IEEE Conference on Decision and Control*, pages 6271–6278. IEEE, 2014.
- [5] Weiye Zhao, Tairan He, and Changliu Liu. Model-free safe control for zero-violation reinforcement learning. In *5th Annual Conference on Robot Learning*, 2021.
- [6] Tong Duy Son and Quan Nguyen. Safety-critical control for non-affine nonlinear systems with application on autonomous vehicle. In *2019 IEEE 58th Conference on Decision and Control (CDC)*, pages 7623–7628. IEEE, 2019.
- [7] Jun Zeng, Bike Zhang, and Koushil Sreenath. Safety-critical model predictive control with discrete-time control barrier function. In *2021 American Control Conference (ACC)*, pages 3882–3889. IEEE, 2021.
- [8] Felix Berkenkamp, Matteo Turchetta, Angela P Schoellig, and Andreas Krause. Safe model-based reinforcement learning with stability guarantees. *arXiv preprint arXiv:1705.08551*, 2017.
- [9] Charles Dawson, Zengyi Qin, Sicun Gao, and Chuchu Fan. Safe nonlinear control using robust neural lyapunov-barrier functions. *arXiv preprint arXiv:2109.06697*, 2021.
- [10] Chang-Soon Kang, Jong-Il Park, Mignon Park, and Jaeho Baek. Novel modeling and control strategies for a hvac system including carbon dioxide control. *Energies*, 7(6):3599–3617, 2014.
- [11] Yonghao Gui, Chung Choo Chung, Frede Blaabjerg, and Mads Graun-gaard Taul. Dynamic extension algorithm-based tracking control of statcom via port-controlled hamiltonian system. *IEEE Transactions on Industrial Informatics*, 16(8):5076–5087, 2019.
- [12] Changliu Liu and Masayoshi Tomizuka. Algorithmic safety measures for intelligent industrial co-robots. In *2016 IEEE International Conference on Robotics and Automation (ICRA)*, pages 3095–3102, Stockholm, Sweden, 2016. IEEE.
- [13] Tianhao Wei and Changliu Liu. Safe Control Algorithms Using Energy Functions: A Uni ed Framework, Benchmark, and New Directions. In *2019 IEEE 58th Conference on Decision and Control (CDC)*, pages 238–243, Nice, France, 2019. IEEE.
- [14] Somil Bansal, Mo Chen, Sylvia Herbert, and Claire J Tomlin. Hamilton-jacobi reachability: A brief overview and recent advances. In *2017 IEEE 56th Annual Conference on Decision and Control (CDC)*, pages 2242–2253. IEEE, 2017.
- [15] Tianhao Wei and Changliu Liu. Safe Control with Neural Network Dynamic Models. *arXiv:2110.01110 [cs, eess]*, 2021.

APPENDIX I

PROOF OF LEMMA 3

Proof. Without DE, it is proved in [13] that $u = u^r - \alpha_1 L_{f^u} \phi$. Take $u_k = u_k^r - \alpha_1 L_{f^u} \phi$ into the safety constraint

$$\frac{\partial \phi}{\partial x} f^x + \frac{\partial \phi}{\partial x} f^u u_k \leq -\eta(\phi). \quad (40)$$

Since the QP problem has a convex cost function and convex constraint, the solution is on the boundary. We get

$$\alpha_1 = \frac{\frac{\partial \phi}{\partial x} f^u u_k^r + \eta(\phi) + \frac{\partial \phi}{\partial x} f^x}{\|L_{f^u} \phi\|^2}. \quad (41)$$

Next, we will prove that the safe input is in the form of $u_{k+1} = u_k^r - \alpha_2 L_{f^u} \phi$ for systems with DE.

Since

$$\frac{\partial \dot{\phi}}{\partial u} = \frac{\partial \phi}{\partial x} \cdot \frac{\partial f}{\partial u} = \frac{\partial \phi}{\partial x} \cdot f^u(x) = L_{f^u} \phi, \quad (42)$$

then from the safety constraint in (13), and the definition of $\bar{u} := \frac{u_{k+1} - u_k}{T_S}$, the safe constraint of u_{k+1} is

$$\begin{aligned} \frac{\partial \phi}{\partial x} \Delta x + K \left(\frac{\partial \dot{\phi}}{\partial x} \Delta x + \frac{\partial \dot{\phi}}{\partial u} \Delta u \right) &\leq -\eta(\bar{\phi}) \\ \Rightarrow \frac{K}{T_S} L_{f^u} \phi u_{k+1} &\leq - \left(\frac{\partial \phi}{\partial x} + K \frac{\partial \dot{\phi}}{\partial x} \right) \Delta x \\ &\quad - \frac{K}{T_S} L_{f^u} \phi u_k - \eta(\bar{\phi}) \end{aligned} \quad (43)$$

Hence, the input u_{k+1} is still constrained in a half space and the safe input is in the form of $u_{k+1} = u_k^r - \alpha_2 L_{f^u} \phi$. With the convex constraint, the solution is on the boundary. Take $u_{k+1} = u_k^r - \alpha_2 L_{f^u} \phi$ into (43), we get

$$\begin{aligned} \alpha_2 = \frac{1}{\|L_{f^u} \phi\|^2} &\left[\frac{\partial \phi}{\partial x} f^u u_k^r + \frac{T_S}{K} \eta(\bar{\phi}) \right. \\ &\left. + T_S \frac{\partial \dot{\phi}}{\partial x} f + \left(\frac{T_S}{K} - 1 \right) \frac{\partial \phi}{\partial x} f^u u_k + \frac{T_S}{K} \frac{\partial \phi}{\partial x} f^x \right] \end{aligned} \quad (44)$$

Recall that $\dot{\phi} = \frac{\partial \phi}{\partial x} (f^x + f^u u_k)$, the difference between α_1 and α_2 is:

$$\begin{aligned} \alpha_1 - \alpha_2 = \frac{1}{\|L_{f^u} \phi\|^2} &\left\{ \left[\delta \left(1 - \frac{T_S}{K} \right) - T_S \frac{\partial \dot{\phi}}{\partial x} f \right] \right. \\ &\left. + \left[\left(1 - \frac{T_S}{K} - \lambda T_S \right) \dot{\phi} + \lambda \left(1 - \frac{T_S}{K} \right) \phi \right] - T_S \lambda \epsilon \right\} \end{aligned} \quad (45)$$

Since $\phi + K \dot{\phi} \geq 0$:

$$\begin{aligned} \left(1 - \frac{T_S}{K} - \lambda T_S \right) \dot{\phi} &+ \lambda \left(1 - \frac{T_S}{K} \right) \phi \\ &\geq - \left(\lambda - \frac{1}{K} + \frac{T_S}{K^2} \right) \dot{\phi}. \end{aligned} \quad (46)$$

Then with (23), (45), and (46), we get the result

$$\alpha_1 - \alpha_2 \geq 0. \quad (47)$$

□

APPENDIX II PROOF OF THEOREM 6

Proof. The tracking object Δx_k^r is dynamically feasible means that the state-tracking problems (18) can be converted into input-tracking problems, i.e., $\exists \bar{u}_k^r \in \bar{U}_b$, s.t.,

$$\frac{\partial f}{\partial x} \Delta x_k + \frac{\partial f}{\partial u} \bar{u}_k^r - \Delta^2 x_k^r = 0, \quad (48)$$

then $u_{k+1} = u_k^r - \alpha_2 L_{f^u} \phi$. As function f is L_2 -smooth, i.e.,

$$\begin{aligned} \|f(\bar{x}_{k+1}) - f(\bar{x}_k) - \langle \nabla f, \bar{x}_{k+1} - \bar{x}_k \rangle \| \\ \leq \frac{L_2}{2} \|\bar{x}_{k+1} - \bar{x}_k\|^2, \end{aligned} \quad (49)$$

and the system dynamics can be rewritten as

$$\begin{aligned} \Delta x_{k+1} &= f(x_{k+1}, u_{k+1}) \\ &= f(x_k, u_k) \\ &\quad + \frac{\partial f}{\partial x}(x_{k+1} - x_k) + \frac{\partial f}{\partial u}(u_{k+1} - u_k) + \Delta_1, \end{aligned} \quad (50)$$

it comes that

$$\|\Delta_1\| \leq \frac{L_2}{2} \|\bar{x}_{k+1} - \bar{x}_k\|^2 \leq \frac{L_2}{2} (f_{\max}^2 + \bar{u}_{\max}^2) T_S^2. \quad (51)$$

Since $\frac{\partial f}{\partial u} = f^u$ and (48), we get

$$\begin{aligned} \frac{\partial f}{\partial x}(x_{k+1} - x_k) &+ \frac{\partial f}{\partial u}(u_{k+1} - u_k) \\ &= \frac{\partial f}{\partial x}(x_{k+1} - x_k) + \frac{\partial f}{\partial u}(u_k^r - u_k + \alpha_2 L_{f^u} \phi) \\ &= \left(\frac{\partial f}{\partial x} \Delta x_k + \frac{\partial f}{\partial u} \Delta u_k^r \right) T_S + \alpha_2 f^u L_{f^u} \phi \\ &= \Delta x_k^r - f(x_k, u_k) + \alpha_2 f^u L_{f^u} \phi. \end{aligned} \quad (52)$$

Then, we can conclude that

$$\Delta_2 = \alpha_2 f^u L_{f^u} \phi. \quad (53)$$

□

APPENDIX III MODIFIED-DYNAMICS MOBILE AGENT SYSTEM

A control-affine mobile agent system is introduced in [2], we modify its dynamics to make it non-control-affine, which helps reveal the effect of our method.

$$\begin{bmatrix} \Delta x \\ \Delta y \\ \Delta v_x \\ \Delta v_y \end{bmatrix} = \begin{bmatrix} v_x \\ v_y \\ f_x \\ f_y \end{bmatrix}, \quad (54)$$

where $[x, y, v_x, v_y]^T$ is the state variable, $f_x = u_x + 0.1 \sin(u_x) + 0.2 u_x \cos(u_x)$, $f_y = u_y + 0.1 \sin(u_y) + 0.2 u_y \cos(u_y)$, and $[u_x, u_y]^T$ is the input variable.